KOREAN JOURNAL OF PACKAGING SCIENCE & TECHNOLOGY
Vol. 26, No. 3 125~131 (2020)
https://doi.org/10.20909/kopast.2020.26.3.125

Preparation of Carrageenan-based Antimicrobial Films Incorporated With Sulfur Nanoparticles

Shahab Saedi, Mastaneh Shokri, and Jong-Whan Rhim*

Department of Food and Nutrition, BioNanocomposite Research Institute, Kyung Hee University, 26 Kyungheedae-ro, Dongdaemun-gu, Seoul 02447, Republic of Korea.

Abstract Carrageenan-based functional films were prepared by adding two different types of sulfur nanoparticles (SNP) synthesized from sodium thiosulfate (SNP^{STS}) and elemental sulfur (SNP^{ES}). The films were characterized using Fourier transform infrared spectroscopy (FT-IR), X-ray diffraction spectroscopy (XRD), and thermal gravimetric analysis (TGA). Also, film properties such as UV-visible light transmittance, water contact angle (WCA), water vapor permeability (WVP), mechanical properties, and antibacterial activity were evaluated. SNPs were uniformly dispersed in the carrageenan matrix to form flexible films. The addition of SNP significantly increased the film properties such as water vapor barrier and surface hydrophobicity but did not affect the mechanical properties. The carrageenan/SNP composite film showed some antibacterial activity against foodborne pathogenic bacteria, *L. monocytogenes* and *E. coli*.

Keywords Carrageenan, Sulfur nanoparticle, Elemental sulfur, Sodium thiosulfate, Antibacterial activity

Introduction

The increasing environmental concerns of plastic waste and the depletion of natural resources have raised interest in renewable polymer-based environmentally-friendly packaging materials. In addition, with the recent increase in demand for safe and high-quality foods by general consumers, the need for functional packaging with antibacterial and antioxidant properties in the food packaging field is also increasing. Accordingly, functional packaging materials based on biopolymers have emerged due to impressive characteristics of biopolymers such as abundant availability, renewability, biodegradability, biocompatibility, and the potential for the development of novel functional composite materials[1]. As one of such bio-polymers, carrageenan has been widely used for the preparation of functional packaging films due to the excellent film-forming property with high mechanical strength[2,3]. Carrageenan is a group of sulfated polysaccharides isolated from cell walls of red seaweed[4,5]. Carrageenan is a linear polymer made up of a repeating disaccharide unit of sulfated galactose and anhydrous-galactose connected via α-1,3 and β-1,4 glycosidic linkages. However, the industrialization of packaging films using carrageenan has been limited due to the inherent hydrophilicity and low physical properties of carrageenan films. As one of the methods of solving the problem of the carrageenan film, a method of manufacturing a functional composite material by adding various types of functional fillers such as AgNP, ZnO NP, and CuO NP has been proposed[2,6,7]. The addition of such nanofillers not only improved the mechanical and gas barrier properties but also provided functional features such as antimicrobial, antioxidant, and UV-barrier properties[2].

Recently, nano-sized sulfur or sulfur nanoparticles (SNP) have been newly suggested for the use as a functional filler for the preparation of functional food packaging films[8,9,10,11]. Sulfur nanoparticles (SNP) have unique chemical properties and biological activities and find extensive applications such as antimicrobial and anticancer agents, pesticide, pharmaceuticals, cosmetics, and synthesis of nanocomposites for lithium batteries[10]. The biological activity of elemental sulfur has long been known, but its hydrophobicity has limited its practical application. However, elemental sulfur is nowadays readily available for aqueous applications in the form of sulfur nanoparticles, which is a convenient solution to extend the biological applications of sulfur[12]. Preparation of sulfur nanoparticles from different sulfur-containing materials such as hydrogen sulfide[13], sodium thiosulfate,[14] and different polysulfide salts[12,15] has been proposed to promote the use of sulfur. Also, a method of preparation of sulfur nanoparticles using low priced elemental sulfur has been developed for the high value-added utilization of the sulfur nanoparticles[12,16].

To date, there are limited reports on the manufacture of

*Corresponding Author : Jong-Whan Rhim

Tel : +82-2-961-2350
E-mail : jwrhim@khu.ac.kr

functional nanocomposite films containing sulfur nanoparticles, in particular no work on the use of carrageenan. Although prepared SNP from sodium thiosulfate has been used for the preparation of bio-nanocomposite films before, the prepared SNP from elemental sulfur has not been employed for this purpose yet.

Hence, the main objectives of this study were to synthesize sulfur nanoparticles using two different sulfur precursors, elemental sulfur and sodium thiosulfate, and to prepare carrageen-based functional composite films incorporated with the sulfur nanoparticles and compare their properties. The effect of sulfur nanoparticles on the film properties such as UV-barrier, mechanical strength, water contact angle, water vapor permeability, and antibacterial activity was evaluated.

Material and methods

1. Materials

Elemental sulfur, sodium sulfide pentahydrate ($Na_2S{\cdot}5H_2O$), acetic acid, and hydrochloric acid were purchased from Daejung Chemicals & Metals Co., Ltd. (Siheung, Gyeonggi-do, Korea). Sodium thiosulfate was obtained from Sigma-Aldrich (St. Louis, MO, USA). Food grade κ-carrageenan and chitosan (CS-001, source: shrimp, viscosity:110 cp in 1% acetic acid solution at 25°C, degree of deacetylation: 90%) were obtained from Fine Agar Co. Ltd. (Damyang, Jeonnam, Korea). Tryptic soy broth (TSB), brain heart infusion broth (BHI), and agar powder were procured from Duksan Pure Chemicals Co. Ltd (Ansan, Gyeonggi-do, Korea). *Escherichia coli* O157: H7 ATCC 43895 and *Listeria monocytogenes* ATCC 15313 were obtained from the Korean Collection for Type Cultures (KCTC, Seoul, Korea). The test bacteria were cultured in TSB and BHI agar media, respectively, and stored at 4°C before testing.

2. Preparation of sulfur nanoparticles

Two different types of sulfur nanoparticles (SNP) were prepared using different sulfur sources, elemental sulfur (SNP^{ES}) and sodium thiosulfate (SNP^{STS}), following the previously described methods[16,17]. For the preparation of the SNP^{ES}, 20 mL of sodium sulfide (1 M) was heated to 100°C, and 1.6 g of molecular sulfur was added and stirred for 1 h. The yellow color of molecular sulfur turned reddish-orange, indicating the formation of polysulfide, then mixed with 40 mL of chitosan solution dissolved in acetic acid (0.5 wt% in 1wt% acetic acid). And added hydrochloric acid solution (18 wt%) to the solution with stirring, then the solution turned milky white and precipitated sulfur nanoparticles. In this process, sulfur nanoparticles are formed following reactions:

$$(x-1)S + Na_2S \rightarrow Na_2S_x \quad (1)$$

$$Na_2S_x + 2HCl \rightarrow 2NaCl + H_2S + (x-1)\ S\downarrow \quad (2)$$

The precipitated SNP was collected by centrifugation at 8000 rpm and washed with distilled water three times, and dried at 50 °C for 24 h, and the SNP obtained was designated SNP^{ES}. For the preparation of SNP^{STS}, 2.482 g of sodium thiosulfate was dissolved in 900 mL of distilled water, added 100 mL of 0.2 N HCl solution with continuous stirring. Then 50 mL of 0.5% (w/v, chitosan/1% acetic acid) was added with stirring for 1 h. The SNP was collected and washed repeatedly and dried at 50°C for 24 h, and the SNP obtained was designated SNP^{STS}. In this process, SNP is formed via the following disproportionation reaction:

$$Na_2S_2O_3 + 2HCl \rightarrow 2NaCl + SO_2 + S\downarrow + H_2O \quad (3)$$

3. Preparation of films

For the preparation of carrageenan/SNP composite films, first 0.08 g of SNP (2 wt% based on carrageenan) was added to 150 mL distilled water containing 1.2 g of glycerol and homogenized using a high shear blender mixer (IKA T50 digital Ultra Turrax, Germany) for 10 min and sonicated using a probe-type sonicator (Model VCX 750, Sonics & Materials Inc., Newtown, CT, USA) for 20 min. Then, 4 g carrageenan was added to the SNP suspension and heated for 30 min at 90°C with vigorous stirring. The film solution was cast on a Teflon-coated glass plate (24 cm × 30 cm) and dried at room temperature. The neat carrageenan film without SNP was prepared following the same procedure. Dried films were kept in a humidity chamber (25°C and 50% RH) before tests. The prepared films were designated Carrageenan, $Carr/SNP^{STS}$, and $Carr/SNP^{ES}$ films, respectively, depending on the types of SNP addition.

4. Characterization of nanoparticles and nano-composite films

4.1. UV-vis spectroscopy

A UV-visible spectrophotometer (Mecasys Optizen POP Series UV/Vis, Seoul, Korea) was used to confirm the formation of SNP and to determine the light transmittance of the film at 280 nm (T_{280}) and 660 nm (T_{660}).

4.2. Morphology

The surface morphology of the film sample, which was vacuum sputter coated with platinum, was observed using a field emission scanning electron microscope (FE-SEM, SU8000, Hitachi Co., Ltd., Matsuda, Japan) with an acceleration voltage of 2 kV and a current of 7.4 μA.

4.3. Fourier transform infrared (FTIR) spectroscopy

Fourier transform infrared (FTIR) spectra of the film sample were recorded using the ATR-FTIR spectrometer (TENSOR 37 Spectrophotometer with OPUS 6.0 software, Billerica, MA, USA) in the range of 4000-400 cm^{-1} with an average resolution of 32 scans at 4 cm^{-1}.

4.4. Thermal stability

The thermal stability of the film sample was evaluated using a thermogravimetric analyzer (Hi-Res TGA 2950, TA Instrument, New Castle, DE, USA) at a heating rate of 10°C/min in the temperature range of 30-600°C under a nitrogen flow of 50 cm^3/min.

4.5. XRD

X-ray diffraction pattern of the film sample was obtained using an XRD diffractometer apparatus (PANalytical X'pert Pro MRD Diffractometer, Amsterdam, Netherlands) operating at the voltage of 40 kV and a current of 40 mA in the range of $2\theta = 5\text{-}80°$

4.6. Surface color

The surface color of the film sample was measured using a Chroma meter (Konica Minolta, CR-400, Tokyo, Japan) with a white color plate ($L = 97.75$, $a = -0.49$, and $b = 1.96$) as a standard background. The Hunter color values (L, a, and b) were taken at five random points on the surface, and the average value was recorded. The total color difference (ΔE) was calculated as follows:

$$\Delta E = [(\Delta L)^2 + (\Delta a)^2 + (\Delta b)^2]^{0.5} \quad (4)$$

where ΔL, Δa, and Δb are the difference between each color values of the standard color plate and film sample, respectively.

4.7. Mechanical properties

The thickness of film samples was measured using a hand-held digital micrometer (Mitutoyo, Model MCD-1 PXF, Mitutoyo Corp. Kawasaki, Japan) with a precision of 0.001 mm.

The mechanical properties such as tensile strength (TS), elongation at break (EB), and elastic modulus (EM) were measured using an Instron Universal Testing Machine (Model 5565, Instron Engineering Corporation, Canton, MA, USA) according to the ASTM Method D 882-88. Film samples were cut into rectangular strips (2.54 cm × 15 cm) using a precision double blade cutter (model LB.02/A, Metrotech, S. A. San Sebastian, Spain). The machine was operated with an initial grip separation of 50 mm and a crosshead speed of 50 mm/min. Fifteen strips were tested for each film, and the average value was presented.

4.8. Water contact angle (WCA)

The water contact angle (WCA) of the film sample was measured using a WCA analyzer (Phoneix 150, Surface Electro Optics Co., Ltd., Kunpo, Korea). A rectangular piece of film (3 cm × 10 cm) was fixed on the horizontal movable stage (Black Teflon coated steel, 7 cm × 11 cm) of the WCA analyzer. The WCA was measured soon after dropping a water drop (~10 μL) using a microsyringe.

4.9. Water vapor permeability (WVP)

The WVP of the film samples was determined gravimetrically according to the ASTM E96-95 standard method. A film sample (7.5 cm × 7.5 cm) was attached to a WVP cup (2.5 cm depth and 6.8 cm diameter) containing 18 mL of distilled water and sealed. The assembled WVP cup was in a humidity chamber (model FX 1077, Jeio Tech Co. Ltd., Ansan, Korea) controlled at 25°C and 50% RH, and the weight of the cup was recorded at 1 h interval for 8?h. The water vapor transmission rate (WVTR, g/m^2.s) was determined from the slope of the weight change of the cup vs. time plot. Then, the WVP (g.m/m^2.Pa.s) of the film was calculated as follows:

$$WVP = (WVTR \times L)/\Delta p \quad (5)$$

Where L was the mean film thickness (m), and Δp was the partial water vapor pressure difference (Pa) across the two sides of the film, which was calculated by the method of Gennadios et al.[18].

4.10. Antibacterial activity

The antibacterial activity of the film samples was evaluated against foodborne pathogenic Gram-positive (*L. monocytogenes*) and Gram-negative (*E. coli*) bacteria using a total viable colony count method[11]. The test bacteria (*L. monocytogenes* and *E. coli*) were aseptically inoculated in the TSB and BHI broth, respectively, and cultured for 16 h at 37°C with mild shaking. The inoculum (10^8-10^9 CFU/mL) was diluted to obtain the bacterial concentration around 10^5-10^6 CFU/mL. 20 mL of the diluted inoculum was aseptically transferred to flasks containing 100 mg of film samples and incubated at 37°C for 12?h with mild shaking at 100 rpm. Samples were taken out from the culture broth every 3 h interval and plated on agar plates after appropriate dilution to determine viable cell counts.

5. Statistical analysis

Film properties were measured with individually prepared films in triplicate as the replicated experimental units, and the results were presented as mean ± SD (standard deviation). One-way analysis of variance (ANOVA) was performed, and the significance of each mean value was determined ($p < 0.05$) with Duncan's multiple range tests using the SPSS software (SPSS Inc., Chicago, IL, USA).

Results and discussion

1. Appearance and surface morphology of the film

The carrageenan and carrageenan/SNP composite films were flexible and transparent. The appearance and surface microstructure of the films are shown in Fig. 1.

The neat carrageenan film was highly transparent without

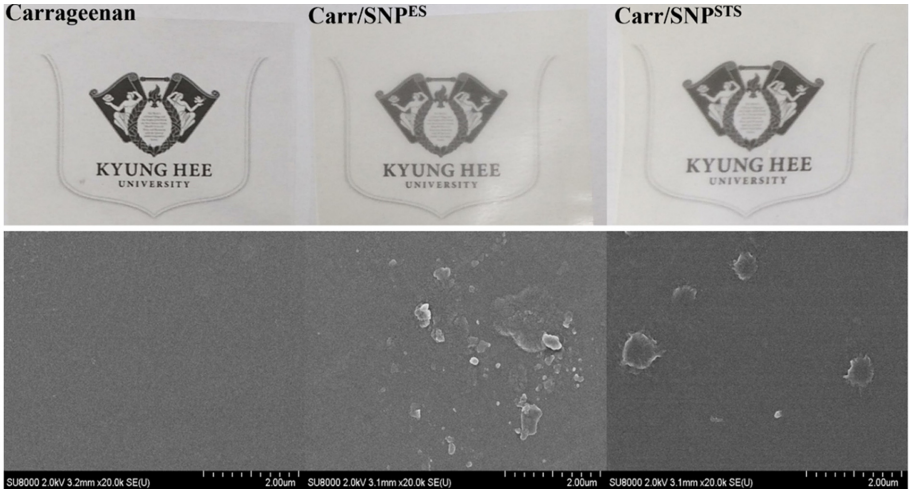

Fig. 1. Appearance and SEM images of the carrageenan-based films.

any color. By the way, the SNP incorporated carrageenan films (Carr/SNP^{STS} and Carr/SNP^{ES}) milky white color with lower transparency than the neat carrageenan film. The decrease in the transparency of the composite films can be due to the light scattering at high wavelengths by the SNP[19]. However, between the two composite films, the Carr/SNP^{STS} film was a little bit more transparent than the Carr/SNP^{ES} film. The lower transparency of Carr/SNP^{ES} may be due to the higher degree of aggregation of SNP^{ES} compared with SNP^{STS} in the polymer matrix, as shown in the SEM images. As shown in the SEM images, the surface of the neat carrageenan film was smooth and intact without any defects. However, the surface of the composite films was slightly rougher than the neat carrageenan film. Due to the hydrophobicity of sulfur, SNPs were not completely dissolved in the hydrophilic polymer matrix but were evenly distributed in the form of nanoparticles.

2. FTIR and XRD

The FTIR test was performed to find the molecular-level interaction between the polymer and the SNPs, and the results are shown in Fig. 2.

The absorption bands at 3325 cm^{-1} and 2905 cm^{-1} were due to the stretching vibration of hydroxyl groups and C-H vibration, respectively. Peaks at 1650 and 1425 cm^{-1} were attributed to the adsorbed water. Absorption bands of the sulfate ester group, C-O bonds of 3,6-anhydro-D-galactose, and C-O-SO_3 of D galactose-4-sulfate appeared at 1220 cm^{-1}, 917 cm^{-1}, and 835 cm^{-1}, respectively.[2] The FTIR results showed that there were no observable changes in the position and peak intensity of the carrageenan film by the addition of SNPs. The FTIR results indicate that there were no significant molecular-level interactions formed between the carrageenan polymer matrix and SNPs[20].

The crystalline nature of the film samples was tested using X-ray diffraction (XRD) analysis, and the XRD patterns of the carrageenan and carrageenan/SNP composite films are shown in Fig. 3.

It has been reported that the SNP has characteristic diffraction peaks in the range of 20-50°[15]. However, the carrageenan/SNP films did not show any additional peaks of

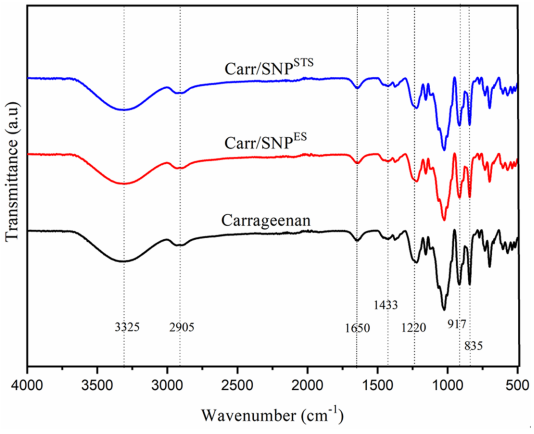

Fig. 2. FT-IR spectra of the carrageenan-based films.

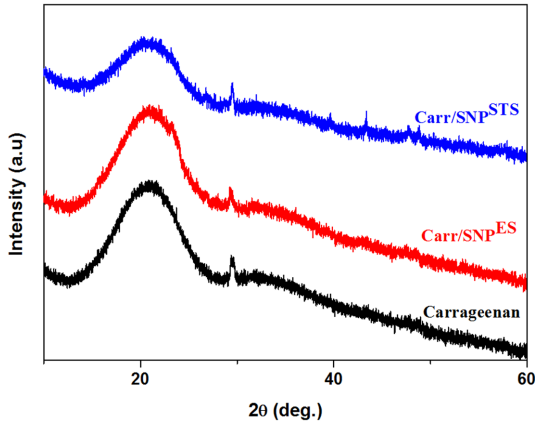

Fig. 3. XRD patterns of the carrageenan-based films.

Table 1. Apparent color and light transmittance of carrageenan-based films

Film	*L*	*a*	*b*	*ΔE*	T_{280} (%)	T_{660} (%)
Carrageenan	91.26 ± 0.12[a]	–0.470.02[c]	5.46 ± 0.18[a]	1.17 ± 0.22[a]	71.8 ± 1.6[c]	90.0 ± 0.4[c]
Carr/SNP^{ES}	91.51 ± 0.05[b]	–0.870.0[a]	7.48 ± 0.09[c]	2.99 ± 0.09[c]	39.4 ± 1.5[a]	47.8 ± 1.3[a]
Carr/SNP^{STS}	91.53 ± 0.01[b]	–0.760.04[b]	6.80 ± 0.22[b]	2.32 ± 0.21[b]	49.6 ± 1.4[b]	64.7 ± 0.7[b]

The values are presented as mean±standard deviation. Any two means in the same column, followed by the same letter are not significantly ($p > 0.05$) different from Duncan's multiple range tests.

SNP compared with the neat carrageenan film. This may be due to the low concentration of SNP, which was embedded inside the polymer[11]. Similarly, the XRD diffraction peaks of SNP were not observed in other biopolymer-based films such as chitosan and alginate films incorporated with an even higher content of SNP (3 wt%) than the current study (2 wt%)[9,11].

3. Optical properties

The surface color and light transmittance of the carrageenan and carrageenan/SNP composite films are shown in Table 1.

The neat carrageenan film was transparent without any color. The addition of sulfur nanoparticles increased lightness (*L*-value) and greenness (decrease in *a*-value) slightly and increased yellowness (*b*-value) significantly, and consequently increased total color difference (*ΔE*) of carrageenan film. The increased greenness and yellowness of the carrageenan/SNP films was due to the slightly yellowish sulfur nanoparticles[11]. tween the SNPs, the effect of SNP^{ES} on the film surface color was more pronounced than that of SNP^{STS}. The higher *b*-value of Carr/SNP^{ES} was probably due to the higher degree of aggregation of SNP^{ES} than SNP^{STS} in the polymer matrix, as observed in the SEM results (Fig. 1).

The light transmittance of the carrageenan film at UV and visible light wavelengths was very high, with the T_{280} and T_{660} of 71.8% and 90%, respectively, indicating that the film is highly transparent to both UV and visible lights. However, the addition of SNPs reduced the light transmittance significantly ($p < 0.05$). The decreased light transmittance of the carrageenan/SNP composite films was mainly due to the light scattering and prevention of light passage by the nano-sized sulfur particles distributed in the polymer matrix[19,3]. The lower light transmittance of the Carr/SNP^{ES} film compared to the carr/SNP^{STS} film was also due to the higher degree of aggregation of SNP^{ES} [3].

4. Mechanical properties

The thickness of the carrageenan and carrageenan/SNP films are shown in Table 2.

The addition of SNPs increased the thickness of the carrageenan film, but the increase was not statistically significant ($p > 0.05$). Similarly, the thickness of the chitosan film to which the same amount of SNP (2.0 wt% based on the polymer) was added as in the current work did not change significantly[11].

Table 2 also shows the mechanical properties such as the tensile strength (TS), elongation at break (EB), and elastic modulus (EM) of the carrageenan and carrageenan/SNP films. The carrageenan film was relatively strong and stiff, with low flexibility. The addition of SNPs did not significantly influence the mechanical properties of the carrageenan film. A similar effect of the addition of SNP was observed in the chitosan-based film[11]. An even distribution of SNP in the polymer matrix and the interaction between them may preserve the mechanical strength of the film to maintain the same level of the mechanical properties.

5. Water contact angle (WCA) and water vapor permeability (WVP)

The surface wettability (or surface hydrophilicity) and water vapor barrier properties of packaging films are usually evaluated by measuring the WCA and WVP of the film, respectively. In order to increase the water-resistance or water vapor barrier of the biopolymer film, a method of adding a hydrophobic nanofiller to a hydrophilic biopolymer is generally used[21]. The WCA and WVP of the carrageenan and carrageenan/SNP films are also shown in Table 2. Typically, a film with a WCA less than 65° is considered as hydrophilic[22]. The WCA of the

Table 2. Mechanical properties, water contact angle, and water vapor permeability of carrageenan-based films

Film	Thickness (μm)	TS (MPa)	EM (MPa)	EB (%)	WCA (°)	WVP ($\times 10^9$ g.m/m^2.Pa.s)
Carrageenan	52.2 ± 5.0[a]	40.9 ± 4.4[a]	1394 ± 211[a]	8.0 ± 2.9[a]	57.2 ± 3.7[a]	1.66 ± 0.13[c]
Carr/SNP^{ES}	55.5 ± 5.0[a]	40.8 ± 4.6[a]	1285 ± 153[a]	8.8 ± 1.7[a]	71.2 ± 2.0[b]	1.29 ± 0.13[a]
Carr/SNP^{STS}	55.1 ± 3.5[a]	42.9 ± 4.7[a]	1365 ± 199[a]	8.1 ± 2.8[a]	70.8 ± 1.4[b]	1.36 ± 0.17[b]

The values are presented as mean±standard deviation. Any two means in the same column, followed by the same letter are not significantly ($p > 0.05$) different from Duncan's multiple range tests.

neat carrageenan film was 57.2°; thus, it is classified as a hydrophilic film as other biopolymer films. However, the WCA of the film increased significantly, up to 72° by the addition of SNP, which can be considered to have a hydrophobic surface. The increased hydrophobicity of the Carr/SNP^{STS} and Carr/SNP^{ES} films was mainly due to the even distribution of the hydrophobic sulfur nanoparticle in the carrageenan polymer matrix[11].

The WVP of the neat carrageenan film was 1.66×10^{-9} g.m./m^2.Pa.s, which is consistent with the previously reported results[2,3]. The addition of SNPs significantly reduced the WVP of the film by 18-22%, depending on the type of SNP. The decrease in the WVP of the carrageenan/SNP composite films was agreed well with the result of the WCA. The reduced WVP of the carrageenan/SNP composite films can be due to the reduced water vapor solubility at the film surface as well as the hindered water vapor diffusional path by the SNP in the polymer matrix[23-25].

6. Thermal stability

The thermal stability of the carrageenan and carrageenan/SNP composite films were tested using TGA, and the results of TGA and DTG thermograms are shown in Fig. 4. The films' thermal degradation occurred at three stages; 80-110°C, 170-220°C, and 220-320°C due to the evaporation of adsorbed water, evaporation of glycerol, and decomposition of carrageenan, respectively. In the first stage of thermal degradation, the difference in weight loss depending on the films was primarily due to their moisture content. In general, the addition of SNP did not influence the thermal stability of the carrageenan film, which was also observed in the chitosan-based film[11].

7. Antibacterial activity

Antibacterial activity of the carrageenan and carrageenan/SNP composite films was evaluated using two foodborne pathogenic bacteria, *E. coli* and *L. monocytogenes,* and results are shown in Fig. 5. Both test bacteria grew logarithmically in the control group containing carrageenan film, but the Gram-positive bacteria (*L. monocytogenes*) grew faster than the Gram-negative bacteria (*E. coli*). *L. monocytogenes* grew initially from 6.3 Log(CFU/mL) to 9.7 Log(CFU/mL) after 12 h of incubation in the carrageenan film containing group, but *E. coli* grew from 6.15 Log(CFU/mL) to 8.8 Log(CFU/mL) for the same incubation time. Compared with the control group, the SNP containing films showed distinctive antibacterial activity depending on the type of test bacteria. The SNP containing films showed more pronounced antibacterial activity against *L. monocytogenes* than *E. coli*., i.e., they showed bacteriostatic activity against *L. monocytogenes* showing 2.1-2.5 Log(CFU/mL) lower than the control group after 12 h of incubation. Still, they showed slightly reduced growth of *E. coli* showing only 0.5-0.7 Log(CFU/mL) lower than that of the control group after 12 h of incubation. Although the antifungal activity of sulfur has been known for a long time, the antibacterial activity of sulfur nanoparticles has not been extensively investigated. Previously, Libenson et al.[26]. showed that small particles of elemental sulfur have antibacterial activity against some Gram-positive bacteria, but most Gram-negative bacteria, including *E. coli*, are resistant against elemental sulfur. They also found that the smaller the particle of elemental sulfur, the better the antibacterial activity. Recently, the antibacterial activity of sulfur nanoparticle has been investigated. Paralikar and Rai[15] reported on the antibacterial activity of SNP against *E. coli* and *S. aureus*. Suleiman et al[27]. reported that Gram-negative bacteria, like *E. coli,* was not inhibited by SNP. Their findings are in good agreement with the current results of the antimicrobial activity of SNPs on the differential activity against Gram-positive and Gram-negative bacteria. As for the type of SNPs, the SNP^{ES}-added film showed slightly higher antimicrobial activity than the SNP^{STS}-added film, but the difference was not significant. It is important to note that SNP^{ES}-added films have similar or higher antimicrobial activity compared to SNP^{STS}-added films. Because SNP^{ES} can be produced in a simple process using inexpensive and abundant elemental sulfur[16], mass production of sulfur nanoparticles for industrial use can be made easily.

The antimicrobial action of sulfur and sulfur nanoparticles has not yet been revealed. Still, explanations have been proposed in which sulfur and SNP react with sulfur-containing enzymes to inactivate these enzymes, thereby releasing toxic hydrogen sulfide gas[26,28].

Conclusions

Two different types of sulfur nanoparticles were synthesized using a different source of sulfur, sodium thiosulfate, and elemental sulfur, and they were used for the preparation of carrageenan-based functional films. The addition of SNPs increased the water vapor barrier and surface hydrophobicity and provided some antibacterial activity but did not affect the mechanical properties of the carrageenan film. Above all, the film properties of the carrageenan film containing SNP were similar regardless of the type of SNP. Therefore, the method of preparing SNPs from elemental sulfur may be used as a more convenient and environmentally friendly method of producing SNPs using an abundant source of elemental sulfur.

Acknowledgment

This work was supported by the National Research Foundation of Korea (NRF) grant funded by the Korea government (MSIT) (No. 2019R1A2C2084221).

References

1. Rhim, J.-W., Park, H.-M., & Ha, C.-S. (2013). Bio-nanocomposites for food packaging applications. Progress in Polymer Science, 38(10-11), 1629-1652.
2. Roy, S., Shankar, S., & Rhim, J.-W. (2019). Melanin-mediated synthesis of silver nanoparticle and its use for the preparation of carrageenan-based antibacterial films. Food Hydrocolloids, 88, 237–246.
3. Saedi, S., & Rhim, J.-W. (2020). Synthesis of Fe_3O_4@ SiO_2@ PAMAM dendrimer@AgNP hybrid nanoparticles for the preparation of carrageenan-based functional nanocomposite film. Food Packaging and Shelf Life, 24, 100473.
4. Campo, V. L., Kawano, D. F., da Silva Jr, D. B., & Carvalho, I. (2009). Carrageenans: Biological properties, chemical modifications and structural analysis - A review. Carbohydrate Polymers, 77(2), 167-180.
5. Usov, A. I. (1998). Structural analysis of red seaweed galactans of agar and carrageenan groups. Food Hydrocolloids, 12(3), 301-308.
6. Kanmani, P., & Rhim, J.-W. (2014a). Properties and characterization of bionanocomposite films prepared with various biopolymers and ZnO nanoparticles. Carbohydrate Polymers, 106, 190-199.
7. Shankar, S., Wang, L.-F., & Rhim, J.-W. (2017). Preparation and properties of carbohydrate-based composite films incorporated with CuO nanoparticles. Carbohydrate Polymers, 169, 264-271.
8. Ezati, P., & Rhim, J.-W. (2020). pH-responsive pectin-based multifunctional films incorporated with curcumin and sulfur nanoparticles. Carbohydrate Polymers, 230, 115638.
9. Priyadarshi, R., Kim, H.-J., & Rhim, J.-W. (2020). Effect of sulfur nanoparticles on properties of alginate-based films for active food packaging applications. Food Hydrocolloids, 106155.
10. Shankar, S., Jaiswal, L., & Rhim, J.-W. (2020). New insight into sulfur nanoparticles: Synthesis and applications. Critical Reviews in Environmental Science and Technology, http://doi.org/10.1080/10643389.2020.1780880
11. Shankar, S., & Rhim, J.-W. (2018). Preparation of sulfur nanoparticle-incorporated antimicrobial chitosan films. Food Hydrocolloids, 82, 116-123.
12. Massalimov, I. A., Shainurova, A. R., Khusainov, A. N., & Mustafin, A. G. (2012). Production of sulfur nanoparticles from aqueous solution of potassium polysulfide. Russian Journal of Applied Chemistry, 85(12), 1832-1837.
13. Deshpande, A. S., Khomane, R. B., Vaidya, B. K., Joshi, R. M., Harle, A. S., & Kulkarni, B. D. (2008). Sulfur nanoparticles synthesis and characterization from H_2S gas, using novel biodegradable iron chelates in W/O microemulsion. Nanoscale Research Letters, 3(6), 221.
14. Chaudhuri, R. G., & Paria, S. (2011). Growth kinetics of sulfur nanoparticles in aqueous surfactant solutions. Journal of Colloid and Interface Science, 354(2), 563-569.
15. Paralikar, P., & Rai, M. (2017). Bio-inspired synthesis of sulphur nanoparticles using leaf extract of four medicinal plants with special reference to their antibacterial activity. IET Nanobiotechnology, 12(1), 25-31.
16. Saedi, S., Shokri, M., & Rhim, J.-W. (2020). Antimicrobial activity of sulfur nanoparticles: Effect of preparation methods. Arabian Journal of Chemistry. 13, 6580-6588.
17. Shankar, S., Pangeni, R., Park, J. W., & Rhim, J.-W. (2018). Preparation of sulfur nanoparticles and their antibacterial activity and cytotoxic effect. Materials Science and Engineering: C, 92, 508-517.
18. Gennadios, A., Weller, C. L., & Gooding, C. H. (1994). Measurement errors in water vapor permeability of highly permeable, hydrophilic edible films. Journal of Food Engineering, 21(4), 395-410.
19. Calvo, M. E., Castro Smirnov, J. R., & Míguez, H. (2012). Novel approaches to flexible visible transparent hybrid films for ultraviolet protection. Journal of Polymer Science Part B: Polymer Physics, 50(14), 945-956.
20. Kanmani, P., & Rhim, J.-W. (2014b). Development and characterization of carrageenan/grapefruit seed extract composite films for active packaging. International Journal of Biological Macromolecules, 68, 258-266.
21. Rhim, J.-W., & Wang, L.-F. (2014). Preparation and characterization of carrageenan-based nanocomposite films reinforced with clay mineral and silver nanoparticles. Applied Clay Science, 97, 174-181.
22. Vogler, E. A. (1998). Structure and reactivity of water at biomaterial surfaces.
23. Advances in Colloid and Interface Science, 74(1-3), 69-117.
24. Shankar, S., Kasapis, S., & Rhim, J.-W. (2018). Alginate-based nanocomposite films reinforced with halloysite nanotubes functionalized by alkali treatment and zinc oxide nanoparticles. International Journal of Biological Macromolecules, 118, 1824-1832.
25. Tang, X., Alavi, S., & Herald, T. J. (2008). Barrier and mechanical properties of starch-clay nanocomposite films. Cereal Chemistry, 85(3), 433-439.
26. Wang, L.-F., & Rhim, J.-W. (2017). Functionalization of halloysite nanotubes for the preparation of carboxymethyl cellulose-based nanocomposite films. Applied Clay Science, 150, 138-146.
27. Libenson, L., Hadley, F. P., McIlroy, A. P., Wetzel, V. M., & Mellon, R. R. (1953). Antibacterial effect of elemental sulfur. The Journal of Infectious Diseases, 93(1), 28-35.
28. Suleiman, M., Al-Masri, M., Al Ali, A., Aref, D., Hussein, A., Saadeddin, I., & Warad, I. (2015). Synthesis of nanosized sulfur nanoparticles and their antibacterial activities. Journal of Materials and Environmental Science, 6(2), 513-518.
29. Rai, M., Ingle, A. P., & Paralikar, P. (2016). Sulfur and sulfur nanoparticles as potential antimicrobials: from traditional medicine to nanomedicine. Expert Review of Anti-Infective Therapy, 14(10), 969-978.

투고: 2020.09.22 / 심사완료: 2020.11.03 / 게재확정: 2020.11.04